Time-resolved catch and release of an optical pulse from a dynamic photonic crystal nanocavity

AUTHOR(S):

Upham, Jeremy; Tanaka, Yoshinori; Kawamoto, Yousuke; Sato, Yoshiya; Nakamura, Tatsuya; Song, Bong Shik; Asano, Takashi; Noda, Susumu

CITATION:

Upham, Jeremy ...[et al]. Time-resolved catch and release of an optical pulse from a dynamic photonic crystal nanocavity. Optics Express 2011, 19(23): 23377.

ISSUE DATE:

2011

URL:

http://hdl.handle.net/2433/151821

Time-resolved catch and release of an optical pulse from a dynamic photonic crystal nanocavity

Jeremy Upham,[1,*] Yoshinori Tanaka,[1] Yousuke Kawamoto,[1] Yoshiya Sato,[1] Tatsuya Nakamura,[1] Bong Shik Song,[1,2] Takashi Asano,[1] and Susumu Noda[1]

[1]*Department of Electronic Science and Engineering, Kyoto University, Katsura, Nishikyo-ku, Kyoto 615-8510, Japan*
[2]*School of Information and Communication Engineering, Sungkyunkwan University, Jangan-Gu Suwon Gyeonggi-do 440-746, South Korea*
[*]*jeremy@qoe.kuee.kyoto-u.ac.jp*

Abstract: We perform time-domain measurements of the interaction between light and silicon photonic crystal nanocavities under dynamic *Q* factor control. Time-resolved evidence of optical pulse capture and release on demand is demonstrated and compared for samples with dynamic *Q* ranges from ~3,000 to 26,000 and from 18,500 to 48,000. Observing the energy behaviour in response to dynamic control provides insight not available with time-integrated measurements into factors influencing device performance such as carrier absorption and pulse capture efficiency.

OCIS codes: (230.5298) Photonic crystals; (230.5750) Resonators; (130.0130) Integrated optics.

References and links

1. Y. Tanaka, J. Upham, T. Nagashima, T. Sugiya, T. Asano, and S. Noda, "Dynamic control of the Q factor in a photonic crystal nanocavity," Nat. Mater. **6**(11), 862–865 (2007).
2. E. J. Reed, M. Soljacić, and J. D. Joannopoulos, "Color of shock waves in photonic crystals," Phys. Rev. Lett. **90**(20), 203904 (2003).
3. J. Upham, Y. Tanaka, T. Asano, and S. Noda, "On-the-fly wavelength conversion of photons by dynamic control of photonic waveguides," Appl. Phys. Express **3**(6), 062001 (2010).
4. C. A. Husko, A. de Rossi, S. Combrié, Q. V. Tran, F. Raineri, and C. W. Wong, "Ultrafast all-optical modulation in GaAs photonic crystal cavities," Appl. Phys. Lett. **94**(2), 021111 (2009).
5. T. Tanabe, M. Notomi, H. Taniyama, and E. Kuramochi, "Dynamic release of trapped light from an ultrahigh-Q nanocavity via adiabatic frequency tuning," Phys. Rev. Lett. **102**(4), 043907 (2009).
6. Y. Tanaka, T. Asano, and S. Noda, "Trapping of ultrashort optical pulse into ultra-high-*Q* photonic nanocavity," in Proceedings of Pacific Rim Conference on Lasers and Electro-Optics (Tokyo, Japan, 2005), 1024–1025.
7. J. Upham, Y. Tanaka, T. Asano, and S. Noda, "Dynamic increase and decrease of photonic crystal nanocavity Q factors for optical pulse control," Opt. Express **16**(26), 21721–21730 (2008).
8. T. Baba, "Slow light in photonic crystals," Nat. Photonics **2**(8), 465–473 (2008).
9. M. F. Yanik and S. Fan, "Stopping light all optically," Phys. Rev. Lett. **92**(8), 083901 (2004).
10. P. E. Barclay, K. Srinivasan, and O. Painter, "Nonlinear response of silicon photonic crystal microresonators excited via an integrated waveguide and fiber taper," Opt. Express **13**(3), 801–820 (2005).
11. T. Nakamura, T. Asano, K. Kojima, T. Kojima, and S. Noda, "Control of emission of quantum dots embedded in photonic crystal nanocavity by manipulating *Q*-factor and detuning," Phys. Rev. B. submitted.
12. K. Hennessy, A. Badolato, M. Winger, D. Gerace, M. Atatüre, S. Gulde, S. Fält, E. L. Hu, and A. Imamoğlu, "Quantum nature of a strongly coupled single quantum dot-cavity system," Nature **445**(7130), 896–899 (2007).
13. Y. Sato, Y. Tanaka, J. Upham, Y. Takahashi, T. Asano and S. Noda, "Strong coupling between distant photonic nanocavities and its dynamic control." (to be published).
14. Y. Akahane, T. Asano, B. S. Song, and S. Noda, "High-*Q* photonic nanocavity in a two-dimensional photonic crystal," Nature **425**(6961), 944–947 (2003).
15. C. Manolatou, M. J. Khan, S. Fan, P. Villeneuve, H. A. Haus, and J. D. Joannopoulos, "Coupling of modes analysis of resonant channel add-drop filters," IEEE J. Quantum Electron. **35**(9), 1322–1331 (1999).
16. B. S. Song, T. Asano, Y. Akahane, and S. Noda, "Role of interfaces in heterophotonic crystals for manipulation of photons," Phys. Rev. B **71**(19), 195101 (2005).
17. S. Jiang, S. Machida, Y. Takiguchi, H. Cao, and Y. Yamamoto, "Wide band AC balanced homodyne detection of weak coherent pulses," Opt. Commun. **145**(1-6), 91–94 (1998).
18. R. Soref and B. Bennett, "Electrooptical effects in silicon," IEEE J. Quantum Electron. **23**(1), 123–129 (1987).

#154397 - $15.00 USD Received 12 Sep 2011; revised 8 Oct 2011; accepted 12 Oct 2011; published 1 Nov 2011

19. D. Dimitropoulos, R. Jhaveri, R. Claps, J. C. S. Woo, and B. Jalali, "Lifetime of photogenerated carriers in silicon-on-insulator rib waveguides," Appl. Phys. Lett. **86**(7), 071115 (2005).
20. A. W. Elshaari, A. Aboketaf, and S. F. Preble, "Controlled storage of light in silicon cavities," Opt. Express **18**(3), 3014–3022 (2010).
21. B. S. Song, S. Noda, T. Asano, and Y. Akahane, "Ultra-high-*Q* photonic double-heterostructure nanocavity," Nat. Mater. **4**(3), 207–210 (2005).
22. T. Tanabe, H. Taniyama, and M. Notomi, "Carrier diffusion and recombination in photonic crystal nanocavity optical switches," J. Lightwave Technol. **26**, 1396–1403 (2008).

1. Introduction

In order to dynamically manipulate the properties of photons, significant effort has gone into combining the precise spatial control of optical modes provided by two-dimensional (2D) photonic crystals (PC) with adroit temporal variation of their characteristics [1–5]. In particular, we have proposed that dynamic control of the Q factor (or photon lifetime) of a PC nanocavity can be used to actively capture light pulses [1,6,7]. By increasing the Q factor of a nanocavity from a low Q state to a high Q state as an optical pulse is coupling into the nanocavity, a significant portion of the pulse can be captured in the resonant mode with a long photon lifetime. The targeted capture of light in resonant modes with wavelength-order modal volumes could be applied to the slowing or stopping photons [8,9], the enhancement of light-matter interaction [10,11] and the manipulation of strong coupling behaviour [12,13]. To date, this dynamic capture has been demonstrated by spectral (i.e., time-integrated) measurements of the nanocavity emission for different relative timings of the dynamic Q factor increase relative to the arrival of the targeted light [1,7], which confirm successful light capture but are not sufficient to properly understand how the photons respond to the manipulated environment. In this work we demonstrate time-resolved measurements of the photons in a nanocavity under dynamic Q control. The Q factor range can be quantifiably measured from the resonant mode decay time and we test different Q ranges to examine their influence on coupling efficiency and carrier absorption losses. Also, we demonstrate the captured light can be released on demand by dynamically lowering the Q factor.

2. Dynamic *Q* control

Figure 1(a) illustrates the system for dynamic control of the Q factor: A nanocavity is coupled to a waveguide that is bound at one end by a reflector. The nanocavity Q factor is determined by two components: the in-plane Q factor (Q_{in}) and the vertical Q factor (Q_V), which are determined by the optical coupling from the nanocavity to the waveguide and to free-space modes, respectively. Q_V is determined by the nanocavity structure itself [14]. For a waveguide open at both ends, Q_{in} would be determined by the nanocavity-waveguide separation (Q_{inO}), but the reflector causes one optical path to double back and interfere with the other. Light propagating along each path will experience a different phase shift, and the phase difference between them (θ) will determine the nature of the interference. Therefore Q_{in} can be manipulated by changing the refractive index of a portion of the waveguide, altering the phase difference between the two optical paths. The total Q factor is then expressed as [1,6,15,16]

$$1/Q = 1/Q_V + (1+\cos\theta)/Q_{in0}. \quad (1)$$

The Q factor can be changed between the minimum $1/(1/Q_V + 2/Q_{in0})$ and the maximum Q_V, by changing θ from 0 to π. When Q_V is designed to be much larger than Q_{in0}, the tuning range can be approximated as between $Q_{in0}/2$ and Q_V. The sequence we propose for dynamic capture and on-demand release of a light pulse is shown in Fig. 1: (a) The initial θ is set to 0. (b) A signal light pulse with a bandwidth corresponding to $Q_{in0}/2$ is injected from the open end of the waveguide. (c) When the light energy in the nanocavity reaches maximum, θ is switched to π. (d) The light energy is preserved in the nanocavity with a loss corresponding to Q_V. (e) At a desired timing, θ is switched to 2π, lowering the Q factor to $Q_{in0}/2$. The light energy is released to the waveguide as a light pulse.

#154397 - $15.00 USD Received 12 Sep 2011; revised 8 Oct 2011; accepted 12 Oct 2011; published 1 Nov 2011

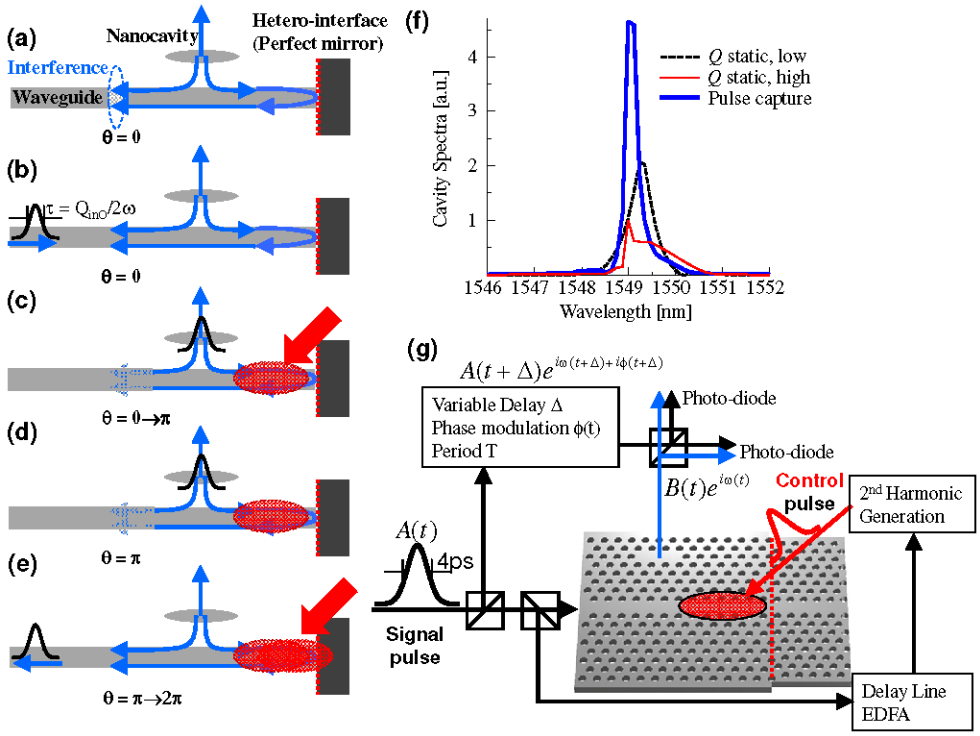

Fig. 1. Schematic of pulse capture and release (a) Sample with an initial phase difference θ = 0. (b) Introduce signal pulse with temporal width matching the *Q* factor. (c) When the signal is in the nanocavity, θ: 0 → π. (d) Light is held in resonant mode with high *Q*. (e) Light is released when θ: π → 2π. (f) Finite difference time domain simulations of nanocavity spectra for the three coupling states: Low, static *Q;* high, static *Q* and dynamic *Q* increase for pulse capture. (g) Schematic of the experimental system for temporal measurements by use of an AC balanced homodyne system. Modulating the reference signal with a known envelope A(t) then convolving it with the vertical emission reveals the temporal envelope of the nanocavity field B(t).

In this scheme, the timing of step (c) is very important: If the signal pulse precedes the dynamic increase of θ from 0 to π, the introduced photons only witness a static, low *Q* state, so light couples to the nanocavity easily, but decouples quickly. If instead the signal pulse arrives after θ has changed to π, it will not couple effectively to the static, high *Q* state, though the small portion of light that does couple to the nanocavity will have a long photon lifetime, corresponding to the high *Q* factor. Pulse capture is only achieved if θ is rapidly changed to π just as the signal pulse is coupling into the nanocavity.

In previous studies [1,7] we investigated the spectrum of the light emitted to free-space for different timings of step (c). Optimal pulse capture is indicated in the spectral domain by maximum peak intensity and minimum spectral width, as the former indicates greater capture efficiency and the latter describes the high *Q* state achieved (Fig. 1(f)). However, the information obtained in the spectral domain is not sufficient to deeply understand the dynamically controlled system because the spectra are time-integrated measurements that cannot describe the photon behaviour response to the dynamic change of the refractive index. Therefore, time-resolved measurements of the photon interaction are necessary to properly investigate such a dynamic system.

3. Samples and experimental set-up

Figure 1 (g) provides a schematic of the samples and experimental setup. The PCs were made from air-suspended 250 nm silicon slabs with a triangular lattice of air holes with lattice

#154397 - $15.00 USD Received 12 Sep 2011; revised 8 Oct 2011; accepted 12 Oct 2011; published 1 Nov 2011

constant a = 407.5 nm and hole radius r = 118 nm. L3 nanocavities with 3 shifted edge holes provide a Q_V of approximately ~50,000 and resonant wavelengths near 1550 nm. A waveguide formed near the nanocavity by a line of filled air holes provides evanescent coupling to the resonant mode. In order to test the behaviour of light under different dynamic Q ranges, we tested samples with different Q_{in0}. Five rows of separation between the waveguide and nanocavity produces a Q_{in0} of ~3,000 (smaller than Q_V), while six rows of separation sets Q_{in0} to ~60,000 (close to Q_V). The in-plane Q factors can be manipulated by interference between the optical paths. The hetero-interface is made by reducing a by 15 nm either 80a, 81a or 82a away from the nanocavity to act as a reflector [16]. Among these samples, one is selected with θ ~0, to minimize the Q factor. For a pulse coupling to the nanocavity, the group velocity in the waveguide is ~0.06c, producing a round trip time between nanocavity and hetero-interface of ~4 ps.

These devices are probed by an optical fiber-based, tunable, passively mode-locked laser (operating wavelength 1535-1555 nm, pulse width ~4 ps) set to the nanocavity resonant wavelength. Pulses from the laser source are split, one portion producing signal pulse input into the PC waveguide, while another is converted to 775 nm pulses by a second harmonic generation crystal and used as control pulses to change the refractive index of the waveguide. When the control pulse strikes the waveguide area, a portion is absorbed by the silicon, generating free carriers. These free carriers lower the refractive index by the plasma effect to change θ. The response time of the refractive index change is set by the temporal width of the 4 ps control pulse.

To observe the interaction of light in the nanocavity evolving over time, we constructed a measurement system based on AC balanced homodyne detection [17]. Another portion of the signal pulses are diverted to form reference pulses, delayed by some time Δ by a variable delay line, then made to interfere with vertical emission from the nanocavity. The interfering output is detected by a balanced photo-detector to cancel out laser intensity noise, and the interfering signal can be further isolated by phase modulating the reference signal (ϕ(t)) and using a lock-in amplifier. The final output is a cross-correlation of the reference pulse with the nanocavity output as a function of Δ, displaying the envelope of the nanocavity amplitude with a resolution of ~4 ps.

4. Measured results and discussion

Figures 2 (a) and (b) show the time-resolved light amplitudes in the nanocavities for samples with Q_{in0} of 3,000 and 60,000, respectively. Three cases are measured for each sample: (1) When the signal pulse enters the nanocavity without a control pulse (black, dashed curve). This case is equivalent to the signal pulse being early and only witnessing the phase difference θ ~0, therefore the curve describes the static, low Q state of the device. (2) When the control pulse arrives before the signal pulse (red curve). In this case the light amplitude behavior describes the static, high Q state (θ = π). (3) When the control pulse arrives just as the light coupling into the nanocavity reaches a maximum (blue, thick curve). Here the light couples into the nanocavity while Q is low, then experiences a dynamic increase of Q. In all cases measuring the exponential decay time (exp(-t/τ)) of the energy in the nanocavity determines the Q factor according to $Q = \omega_o\tau$. Note that the cross-correlation signal actually plots the nanocavity field amplitude over time, rather then energy, so the figures exhibit a decay rate corresponding to 2τ. In Fig. 2 (a), the black curve exhibits rapid decay (τ < 2 ps) suggesting the low Q state (~Q_{in0}/2) is less than 3,000. The measurement of short photon lifetimes are limited by the temporal resolution of the balanced homodyne system, but Q ~3,000 is consistent with spectral measurements of the sample. After the rapid decay of amplitude due to the low Q condition, some smaller peaks are visible for a short time. These are likely due to the light traveling back along the waveguide being partially reflected at the input facet, exhibiting behaviour similar to Fabry-Perot oscillations. They are thus attributable to the fabricated input facet and waveguide length rather than the Q control system design. In Fig. 2(b) the low Q value is 18,500 (τ = 15 ps), which is the minimum value of Q for this sample according to Eq. (1). Next we consider the static, high Q case (red). For both samples

#154397 - $15.00 USD Received 12 Sep 2011; revised 8 Oct 2011; accepted 12 Oct 2011; published 1 Nov 2011

the mismatch between the signal pulse and the spectral width of the resonant mode inhibit the signal pulse from coupling to the high Q state as well as in the low Q case. Nevertheless, the upper bound of the dynamic Q ranges can be measured as 26,000 (τ = 21.5 ps) in Fig. 2(a) and 48,000 (τ = 39.5 ps) in Fig. 2(b). Finally, we examine the response when the control pulse dynamically increases the Q factor just as the field coupled to the nanocavity reaches a maximum (blue). For both samples, the initial coupling to the nanocavity described by the peak amplitude in the nanocavity is very close to that of the static, low Q condition while the decay rate matches the static, high Q condition. Therefore the time-resolved measurements confirm that dynamic Q factor control successfully combines the more effective initial coupling of a low Q with the longer photon lifetime of a high Q to achieve pulse capture. The small decay seen before capture is set in Fig. 2(a) suggests that some light escapes before capture is established because the decay rate to the waveguide ($\tau_{in0} = Q_{in0}/\omega_o$) is close to the roundtrip time. To change θ from 0 to π, ~2 pJ from the control pulse is absorbed along ~10 μm of the waveguide, exciting free carriers with an estimated mean density of 6 x 10^{18} cm^{-3} to reduce the refractive index by ~0.3%.

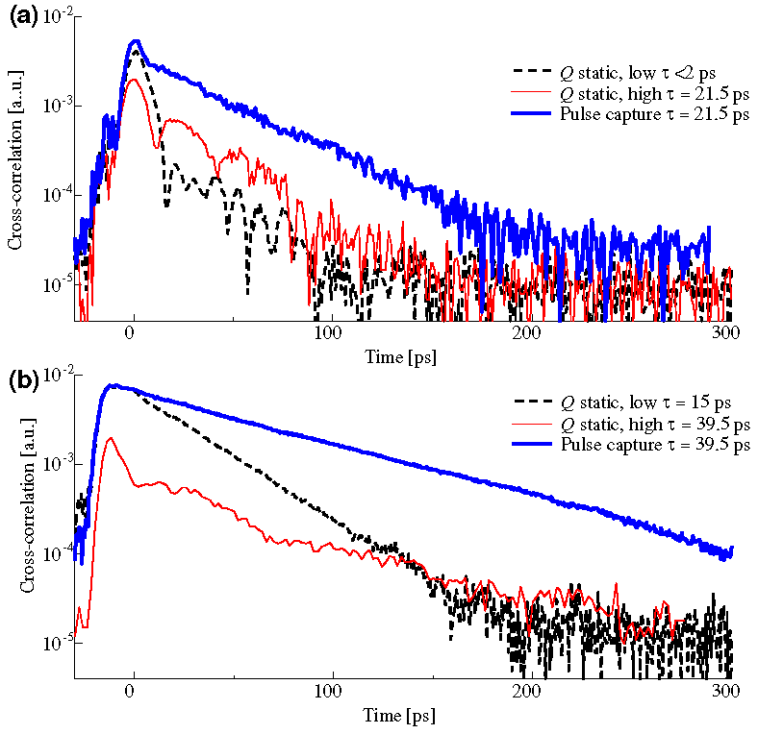

Fig. 2. Time-resolved measurements of the nanocavity field behaviour for high Q, low Q and dynamic Q increase (a) A sample with Q_{inO} ~3,000 is better matched for effective initial coupling of the 4 ps signal pulse. (b) A sample with Q_{inO} = 60,000 showing a higher maximum Q.

Given that both samples use the same type of nanocavity with a Q_V of ~50,000, the measured maximum and minimum Q values for the Q_{in0} = 60,000 sample match closely to the Q range according to Eq. (1). However, in the Q_{in0} ~3,000 case the upper bound of the dynamic Q range is significantly smaller, despite having the same Q_V. This discrepancy is in part due to the resonant mode being used to capture light consisting of not only the nanocavity, but also the field in the waveguide extending to the hetero-interface. In the high Q condition ($\theta = \pi$), a portion of the resonant mode is coupled to the waveguide between the nanocavity and hetero-interface mirror to produce destructive interference. The portion of the

#154397 - $15.00 USD Received 12 Sep 2011; revised 8 Oct 2011; accepted 12 Oct 2011; published 1 Nov 2011

captured light in the waveguide, and thus the modal volume, depend on Q_{in0} [7]. However the free carriers excited by the control pulse will absorb light traveling through this region.

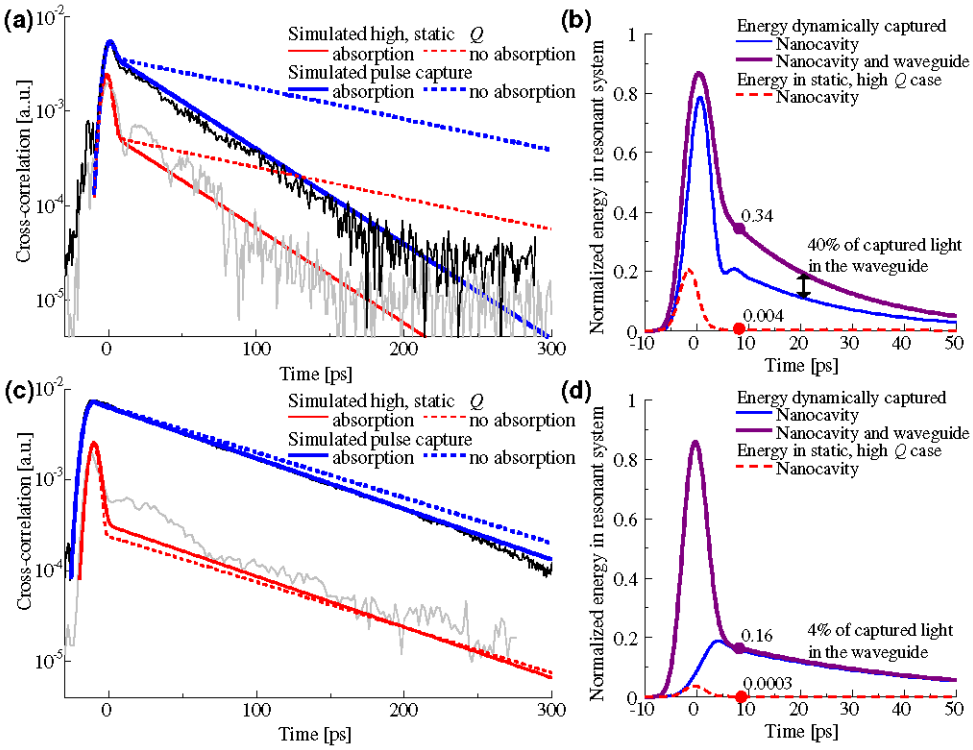

Fig. 3. Coupled mode theory of the nanocavity field over time fit to the experiment. (a) For the Q_{in0} ~3,000 case, light behaviour with (solid lines) and without (dashed lines) free carrier absorption are compared and (b) the energy in the nanocavity and the entire modal volume are simulated to appraise pulse capture efficiency. (c),(d) Same analysis of the Q_{in0} = 60,000 case.

Figure 3 shows coupled mode theory simulations of the device performance (the model is described in the appendix). Simulations of the nanocavity field amplitudes over time, convolved with a 4 ps reference pulse, accurately mimic the measurements of the Q_{in0} ~3,000 (Q_{in0} = 60,000) case in Fig. 3(a) (Fig. 3(c)). The simulations are performed in the presence (solid lines) and absence (dashed lines) of free carrier absorption, which fits the experimental data when equivalent to an absorption coefficient of 44.5 cm^{-1} over 10 μm of the waveguide. This absorption coefficient is slightly lower than predicted in the literature (87 cm^{-1} for carrier density of 6 x 10^{18} cm^{-3} in bulk silicon [18,19]), but this is conceivable for a thin, air-clad waveguide. The simulations suggest that carrier absorption is a significantly stronger inhibitor of high Q in the Q_{in0} ~3,000 device. Examining both the amount of energy in the nanocavity and between it and the hetero-interface (Fig. 3(b)) indicates that ~40% of the captured energy is in the waveguide at any given time, where it is susceptible to free carrier losses. Conversely, in the Q_{in0} = 60,000 device only 4% of the captured energy is in the waveguide (Fig. 3(d)), so this loss impacts the photon lifetime less. Thus the influence of free carrier losses can be significantly weakened by reducing the portion of captured light necessary to maintain the $\theta = \pi$ condition. A similar strategy has been employed in a dynamic coupled ring resonators system by adding additional rings to distance the resonant mode from free carriers [20].

Simulating the time-resolved photon behaviour also permits estimation of each device's pulse capture efficiency. The Q_{in0} = 60,000 sample has a longer photon lifetime, but the mismatch of the minimum Q value and the 4 ps signal pulse lead to only 16% of the signal

#154397 - $15.00 USD Received 12 Sep 2011; revised 8 Oct 2011; accepted 12 Oct 2011; published 1 Nov 2011

pulse energy being in the resonant mode when pulse capture achieves high Q (Fig. 3 (d)). This is still a significant gain over the coupling efficiency of the static, high Q state that retains only 0.03% of the original signal pulse. When Q_{in0} = 3,000, there is better spectral matching between the low Q case, so 34% of the total signal energy introduced is dynamically captured compared to 0.4% for static high Q (Fig. 3(b)). However before the dynamic capture is realized, as much as 79% of the signal pulse energy is in the nanocavity and much of the remainder is in the waveguide between the nanocavity and hetero-interface. Some of this light leaves the nanocavity before the high Q state can be established, causing the peak seen in the dynamic Q case of Figs. 2(a) and 3(a) before being dynamically changed to the long decay rate. This implies that the majority of the energy might be captured if the high Q state could be established more quickly. As a whole, these results suggest that the critical design conditions for effective pulse capture are: (1) Carefully matching of the initial Q condition to the targeted signal pulse for good initial coupling, (e.g., Q_{inO} ~3,000 for a 4 ps signal pulse). (2) A fast transition of θ, which will require reducing both the roundtrip time between the nanocavity and hetero-interface and the transition time from low Q to high Q by the control pulse, relative to the temporal width of the signal pulse (e.g., altering the waveguide mode for a faster group velocity and employing shorter control pulses) (3) A high Q_V (e.g. hetero-structure nanocavities [21]) and minimizing absorption losses for a long photon lifetime.

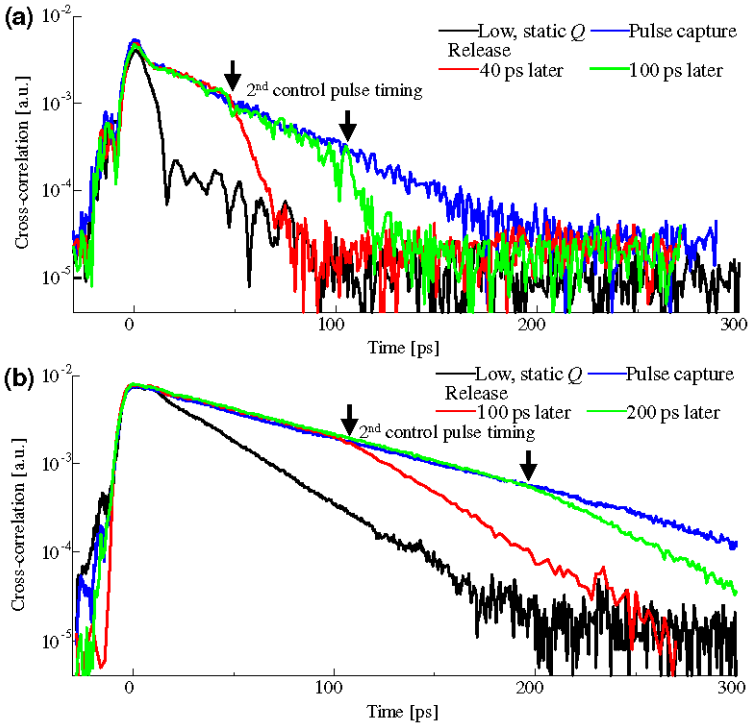

Fig. 4. Time-resolved demonstration of the catch and subsequent release of light from the nanocavity on demand. (a) Q_{inO} ~3,000 (b) Q_{inO} = 60,000.

Finally, multiple dynamic transitions can also be investigated by time-resolved measurements. We repeat the pulse capture experiments, now striking the waveguide with an additional control pulse some time after pulse capture. The second control pulse power can be tuned to shift θ from π to 2π, once again lowering Q at a time of our choosing [7]. The time-resolved measurements in Fig. 4(a) and (b) show the light in the nanocavity being captured, then the photon lifetime suddenly decreasing with the arrival of the second control pulse.

For both cases the decay rate of the nanocavity field suggests that the Q has been returned to its minimum value (i.e., θ ~2π). It should be noted that this final Q state will determine the

#154397 - $15.00 USD Received 12 Sep 2011; revised 8 Oct 2011; accepted 12 Oct 2011; published 1 Nov 2011

temporal width the released pulse. In the Q_{in0} ~3,000 case, the pulse width will be similar to the 4 ps signal pulse introduced because the lifetime is of a similar order, however in the Q_{in0} = 60,000 case the decay rate of 15 ps will produce a pulse with a trailing edge of the same decay rate. Releasing a pulse with the same shape as the input signal would require special attention to both the rate of the dynamic change and the final Q value. Nevertheless these results provide time-resolved evidence of the signal pulse being captured and released on demand.

5. Conclusion

In summary, we investigated the evolution of light behaviour during the capture and release of optical pulses from a PC nanocavity system by dynamic Q factor control via time-resolved measurements. This provided quantifiable insights into device performance including accurate measurements of the dynamic Q range, pulse capture efficiency and the impact of free carrier losses. The dynamic catch and release of light from a PC nanocavity has obvious potential for application to the slowing and stopping of light, as well as enhanced light-matter interaction and the manipulation of strong coupling. In an effort to improve the capture efficiency and photon lifetime of these devices, observing the evolution of photon behaviour provides insight into how different parameters affect the coupling efficiency and photon lifetime. The time-resolved measurement approach will be important in appraising the performance of dynamic devices as further advances such as using nanocavities with intrinsically higher Q_V, the capture and release of light through designated outputs, and novel forms of dynamic control are developed.

6. Appendix

It has been demonstrated that coupled mode theory can model the behaviour of light in a system of interacting resonant and propagating modes [15]. We use this approach to model our dynamic Q control device (Fig. 5).

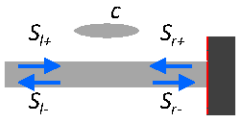

Fig. 5. Schematic of coupled mode theory model used to simulate our device. The field amplitude in the nanocavity c interacts with the incoming and outgoing waves from the from a left port ($S_{l\pm}$) and right port ($S_{r\pm}$).

This model simulates the amplitude of the field in the resonator, c, as it interacts with the field amplitude of propagating modes in the waveguide coming and going from a left port ($S_{l\pm}$) and right port ($S_{r\pm}$):

$$\begin{aligned}
\frac{\mathrm{d}c(t)}{\mathrm{d}t} &= \left(j\omega_o - \frac{1}{2\tau_v} - \frac{1}{2\tau_{in0}} \right) c(t) + \kappa_{in0} S_{l+}(t) + \kappa_{in0} S_{r+}(t) \\
S_{r-}(t) &= S_{l+}(t) - \kappa_{in0}^{*} c(t) \\
S_{l-}(t) &= S_{r+}(t) - \kappa_{in0}^{*} c(t)
\end{aligned} \tag{2}$$

Here ω_o is the resonant frequency of the nanocavity, $\tau_v = Q_V/\omega_o$ and $\tau_{in0} = Q_{in0}/\omega_o$ are the decay rates of energy in the nanocavity to free space modes and the waveguide, respectively. The coupling coefficient between the waveguide and nanocavity $\kappa_{in0,}$ is related to the decay rate according to:

$$\left|\kappa_{in0}\right|^2 = \frac{1}{2\tau_{in0}} \tag{3}$$

#154397 - $15.00 USD Received 12 Sep 2011; revised 8 Oct 2011; accepted 12 Oct 2011; published 1 Nov 2011

In order to describe the interference between modes responsible for manipulating the Q factor, the incoming field amplitude from the right port (S_{r+}) is calculated by delaying the outgoing field (S_{r-}) by the roundtrip time T_p that is calculated from the waveguide length and the group velocity of the signal pulse centered at ω_o. The dispersion of light traveling in the waveguide is not accounted for in this model. To simulate dynamic control by a control pulse, (S_{r+}) is manipulated over 4 ps to change the phase difference from 0 to π. Free carrier absorption can be modeled by attenuating $S_{r+}(t)$ to fit the experimental data. The lifetime of free carriers excited in these air-clad, silicon samples (> 1 ns [22]) is significantly longer than the time scales under investigation, so we neglect the influence of carrier recombination. Once this model is established we can simulate the energy in the nanocavity by $|a|^2$ or the power traveling through different ports by $|S_{l(r)\ \pm}|^2$. Alternatively the field amplitudes can be convolved with a reference pulse to simulate balanced homodyne measurements.

Acknowledgements

This work was supported mainly by Grant-in-Aid for Scientific Research (S) and partially by the Global COE Program of MEXT, Japan, and also partly by JSPS through the FIRST Program initiated by CSTP.

#154397 - $15.00 USD Received 12 Sep 2011; revised 8 Oct 2011; accepted 12 Oct 2011; published 1 Nov 2011